

Dynamic relocation of the TORC1–Gtr1/2–Ego1/2/3 complex is regulated by Gtr1 and Gtr2

Shintaro Kira^a, Yuri Kumano^b, Hirofumi Ukai^b, Eigo Takeda^c, Akira Matsuura^c, and Takeshi Noda^{a,b}

^aCenter for Frontier Oral Science, Graduate School of Dentistry, and ^bGraduate School of Frontier BioSciences, Osaka University, Osaka 565-0871, Japan; ^cDepartment of Nanobiology, Graduate School of Advanced Integration Science, Chiba University, Chiba 263-8522, Japan

ABSTRACT TORC1 regulates cellular growth, metabolism, and autophagy by integrating various signals, including nutrient availability, through the small GTPases RagA/B/C/D in mammals and Gtr1/2 in budding yeast. Rag/Gtr is anchored to the lysosomal/vacuolar membrane by the scaffold protein complex Ragulator/Ego. Here we show that Ego consists of Ego1 and Ego3, and novel subunit Ego2. The Δ ego2 mutant exhibited only partial defects both in Gtr1-dependent TORC1 activation and Gtr1 localization on the vacuole. Ego1/2/3, Gtr1/2, and Tor1/Tco89 were colocalized on the vacuole and associated puncta. When Gtr1 was in its GTP-bound form and TORC1 was active, these proteins were preferentially localized on the vacuolar membrane, whereas when Gtr1 was in its GDP-bound form, they were mostly localized on the puncta. The localization of TORC1 to puncta was further facilitated by direct binding to Gtr2, which is involved in suppression of TORC1 activity. Thus regulation of TORC1 activity through Gtr1/Gtr2 is tightly coupled to the dynamic relocation of these proteins.

Monitoring Editor

John York
Vanderbilt University

Received: Jul 8, 2015

Revised: Nov 13, 2015

Accepted: Nov 19, 2015

INTRODUCTION

Living organisms must sense nutrient availability to finely modulate their anabolic and catabolic processes and adjust to various environments. Amino acid availability signals are sensed through multiple mechanisms, including the SPS, GCN2, and target of rapamycin complex 1 (TORC1) pathways (Wek *et al.*, 1995; Hara *et al.*, 1998; Ljungdahl, 2009). TORC1 is a multisubunit protein kinase complex conserved from yeast to mammals: in the yeast *Saccharomyces cerevisiae*, TORC1 consists of Tor1 or Tor2, Kog1, Lst8, and Tco89, whereas mammalian TORC1 contains mTor, Raptor, mLst8, Deptor, and PRAS40 (Loewith *et al.*, 2002; Sancak *et al.*, 2007; Peterson *et al.*, 2009). By integrating stimuli such as energy level, stress, and hormonal signals in addition to nutrient availability, TORC1 regu-

lates fundamental processes involved in cellular growth, such as translation, ribosomal biogenesis, and autophagy (Chantranupong *et al.*, 2015; Efeyan *et al.*, 2015).

TORC1 is regulated by heterodimeric small GTPases, RagA/B–RagC/D in mammals and Gtr1/Gtr2 in budding yeast (Hirose *et al.*, 1998; Sekiguchi *et al.*, 2001; Binda *et al.*, 2009; Jewell *et al.*, 2013). When RagA/B and Gtr1 are in their GTP-bound forms, they bind directly to TORC1 (Sancak *et al.*, 2008; Sekiguchi *et al.*, 2014). In mammals, this binding recruits mTORC1 to the lysosome surface and allows it to associate with its activator Rheb, another small GTPase (Sancak *et al.*, 2010). Thus the dynamic relocation of mTORC1 underlies its regulatory mechanism. By contrast, it is not known whether the budding yeast Rheb homologue also serves as a TORC1 activator and, if so, how the activation is achieved (Urano *et al.*, 2000). In addition, we observed that relocation of yeast Tor1 from the vacuolar membrane to other sites in response to nitrogen starvation is not as dramatic: under these conditions, the percentage of cells with vacuole-associated Tor1 decreases from 60 to 39% (Kira *et al.*, 2014). Therefore it remains unclear how the regulation of yeast TORC1 activity is related to its localization.

The RagA/B/C/D complex is anchored to the lysosomal membrane via a scaffold protein complex called Ragulator (Sancak *et al.*, 2010), which consists of p18/Lamtor1, p14/Lamtor2, MP1/Lamtor3, C7orf59/Lamtor4, and HBXIP/Lamtor5 (Sancak *et al.*, 2010);

This article was published online ahead of print in MBoC in Press (<http://www.molbiolcell.org/cgi/doi/10.1091/mbc.E15-07-0470>) on November 25, 2015.

Address correspondence to: Takeshi Noda (takenoda@dent.osaka-u.ac.jp).

Abbreviations used: ALP, alkaline phosphatase; GBP, GFP-binding protein; NTCB, 2-nitro-5-thiocyanatobenzoic acid; TAP, tandem affinity purification; TORC1, target of rapamycin complex 1; WT, wild type.

© 2016 Kira *et al.* This article is distributed by The American Society for Cell Biology under license from the author(s). Two months after publication it is available to the public under an Attribution–Noncommercial–Share Alike 3.0 Unported Creative Commons License (<http://creativecommons.org/licenses/by-nc-sa/3.0>).

“ASCB®,” “The American Society for Cell Biology®,” and “Molecular Biology of the Cell®” are registered trademarks of The American Society for Cell Biology.

Bar-Peled *et al.*, 2012). Ragulator also functions as a guanine nucleotide exchange factor for RagA/B and thus plays a key role in the regulation of Rag and mTORC1 activity (Bar-Peled *et al.*, 2012). The budding yeast counterpart of Ragulator is Ego, which contains at least three molecules: Ego1 and an Ego3 dimer (Dubouloz *et al.*, 2005; Gao and Kaiser, 2006; Zhang *et al.*, 2012). It remains unknown whether yeast Ego is structurally similar to Ragulator. Here we show that the uncharacterized protein Ycr075w-a is novel subunit of Ego. By characterizing its properties, we show that the Ego/Gtr/Tor1 complex is dynamically relocated according to the nucleotide-bound state of Gtr1 and Gtr2.

RESULTS

Identification of Ego2 as a novel subunit of Ego

Yeast Ego is believed to consist of at least three subunits (one molecule of Ego1 protein and an Ego3 dimer), whereas mammalian Ragulator possesses five subunits (Bar-Peled *et al.*, 2012). A recent analysis using HHPred software predicted that mammalian C7orf59 and HBXIP have secondary structure organization similar to that of two uncharacterized yeast proteins, Ycr075w-a and Ynr034w-a (Levine *et al.*, 2013). Hence we examined the relationship between Ycr075w-a and Ynr034w-a and the other yeast Ego subunits. During the review period after the original submission of our manuscript, Powis *et al.* (2015) reported their characterization of these proteins. On the basis of their findings and the results we describe later, we will refer to Ycr075w-a as Ego2.

C-terminally green fluorescent protein (GFP)-tagged Ego1 localizes on the vacuolar membrane and perivacuolar foci (Figure 1A; Binda *et al.*, 2009). This pattern was also observed for Ego2-GFP (Figure 1A). When Ego3 was C-terminally tagged with 3xmCherry fluorescence protein, it colocalized with Ego1-GFP not only on the vacuolar membrane, but also on perivacuolar foci; a similar colocalization was observed for Ego2-GFP (Figure 1A). This pattern of Ego2-GFP localization was completely lost in $\Delta ego1$ mutant cells, and only faint signals remained on the vacuole in $\Delta ego3$ (Figure 1B). Similarly, proper localization of Ego3 required both Ego1 and Ego2 (Figure 1C). By contrast, Ego1 localization on vacuolar membrane was maintained even in $\Delta ego2$ and $\Delta ego3$ mutants (Figure 1D). Ego1 possesses a possible myristoylation sequence (MGXXS/T) at the N-terminal SH4 domain (Ashrafi *et al.*, 1998). In fact, a glycine-to-alanine point mutation in the sequence resulted in a dramatic loss of vacuolar localization (Figure 1E), indicating that it is directly anchored to the vacuole via its lipid modification. On the basis of these results, we postulate that Ego3 and Ego2 are anchored to the vacuolar membrane via Ego1, and Ego2 and Ego3 stabilize each other's association to Ego1.

To determine whether Ego2 is directly associated with Ego1, we performed yeast two-hybrid analysis. Robust positive signals were observed with the combination of either AD or BD vectors (Figure 2A). Furthermore, Ego2-GFP could be pulled down by Ego1-tandem affinity purification (TAP) from lysate of wild-type (WT) yeast but not $\Delta ego3$ mutant cells (Figure 2B). These observations suggest that Ego2 is directly associated with Ego1 and that Ego3 stabilizes the Ego1-Ego2 interaction. Similarly, we detected robust direct interaction between Ego1 and Ego3, as previously reported (Supplemental Figure S1; Zhang *et al.*, 2012). Ego3-GFP could be pulled down by Ego1-TAP in WT yeast but not in $\Delta ego2$ mutant cells (Figure 2C). On the other hand, the two-hybrid interaction between Ego3 and Ego2 was weak and detectable in only one AD/BD combination (Figure 2A). Ego3-GFP could be pulled down by Ego2-TAP, but this interaction was lost in the $\Delta ego1$ mutant (Figure 2D). Together these findings suggest

that the interaction between Ego3 and Ego2 depends on Ego1 and that Ego2 is a novel subunit of Ego.

Ego2 mutants are partially defective in TORC1 activation

Growth of *ego* mutants was sensitive to the TORC1 inhibitor rapamycin (Figure 3A; Binda *et al.*, 2009). The $\Delta ego2$ mutant also exhibited some growth sensitivity to rapamycin relative to the parental WT strain, although this effect was weaker than in the $\Delta gtr1$, $\Delta ego1$, and $\Delta ego3$ mutants (Figure 3A). Gtr1 is kept as a GTP-bound form in the mutant of *NPR2*, a subunit of the SEACIT complex, which has GTPase activation protein (GAP) activity toward Gtr1, leading to persistent activation of TORC1 (Bar-Peled *et al.*, 2013; Panchaud *et al.*, 2013a,b; Kira *et al.*, 2014). The $\Delta gtr1\Delta npr2$, $\Delta ego1\Delta npr2$, and $\Delta ego3\Delta npr2$ double-deletion mutants exhibited rapamycin sensitivity comparable to that of the single-deletion mutants of $\Delta gtr1$, $\Delta ego1$, and $\Delta ego3$, consistent with lack of Gtr1 function in these mutants (Figure 3A). On the contrary, $\Delta ego2\Delta npr2$ cells did not show such severe sensitivity, implying that Gtr1 activity somehow remains.

The $\Delta ego1$ and $\Delta ego3$ mutants were defective in recovery from the growth arrest caused by rapamycin treatment (Dubouloz *et al.*, 2005; Figure 3A). However, the growth of $\Delta ego2$ cells recovered as efficiently as that of WT cells (Figure 3A). In addition, recovery from rapamycin-induced growth arrest was apparent in $\Delta ego2\Delta npr2$ cells, in contrast to $\Delta ego1\Delta npr2$ or $\Delta ego3\Delta npr2$ cells, supporting the idea that some Gtr1 function (and Gtr1-dependent TORC1 activation) persists in $\Delta ego2$ cells.

Next we examined the phosphorylation of Sch9, the substrate of TORC1 kinase, in $\Delta ego2$ cells. Immunoblotting after 2-nitro-5-thiocyanatobenzoic acid (NTCB) treatment to enhance the phosphorylation-dependent mobility shift revealed dephosphorylation of Sch9 upon rapamycin treatment or starvation (Urban *et al.*, 2007). As reported previously, even under nutrient-rich conditions without rapamycin treatment, partial dephosphorylation was observed in $\Delta gtr1$ and $\Delta ego1$ cells relative to WT cells (Figure 3B; Binda *et al.*, 2009). By contrast, in $\Delta ego2$ cells, such significant dephosphorylation was not evident (Figure 3B). We also examined Gtr1-dependent TORC1 activation by monitoring autophagy using an alkaline phosphatase (ALP) assay (Noda *et al.*, 1995; Noda and Ohsumi, 1998; Noda and Klionsky, 2008). In $\Delta npr2$ cells, even under nitrogen starvation, which induces autophagy through TORC1 inactivation in WT cells, autophagy was not induced (Figure 3C; Kira *et al.*, 2014). Accordingly, in the absence of Gtr1, TORC1 could not be activated in $\Delta npr2$ cells, and autophagy was induced normally by nitrogen starvation (Figure 3C; Kira *et al.*, 2014). Deletion of *EGO1* in $\Delta npr2$ cells had the same effect as the *GTR1* deletion, reflecting complete loss of Gtr1 function (Figure 3C). However, deletion of *EGO2* in $\Delta npr2$ cells resulted in only partial induction of autophagy (Figure 3C). Overproduction of the Gtr1-GTP mutant failed to suppress autophagy in $\Delta ego1$ cells but achieved partial suppression in $\Delta ego2$ cells (Figure 3D). Taken together, these data indicate that Gtr1-dependent TORC1 activation was only partially defective in $\Delta ego2$ cells.

On the other hand, a mutant in Ynr034w-a/Ego4, another candidate Ego subunit (Levine *et al.*, 2013; Powis *et al.*, 2015), was not more sensitive to rapamycin than WT cells, and the $\Delta ego4\Delta ego2$ double mutant did not exhibit higher rapamycin sensitivity than the $\Delta ego2$ single mutant (Figure 3A). Furthermore, we detected no two-hybrid interactions between Ego4 and Ego1, Ego3, or Ego2 (Supplemental Figure S1A, top), and neither C-terminally nor N-terminally GFP-tagged Ego4 was localized on the vacuole (Supplemental Figure S1B; unpublished data). These data suggest that Ego4 is not a subunit of Ego.

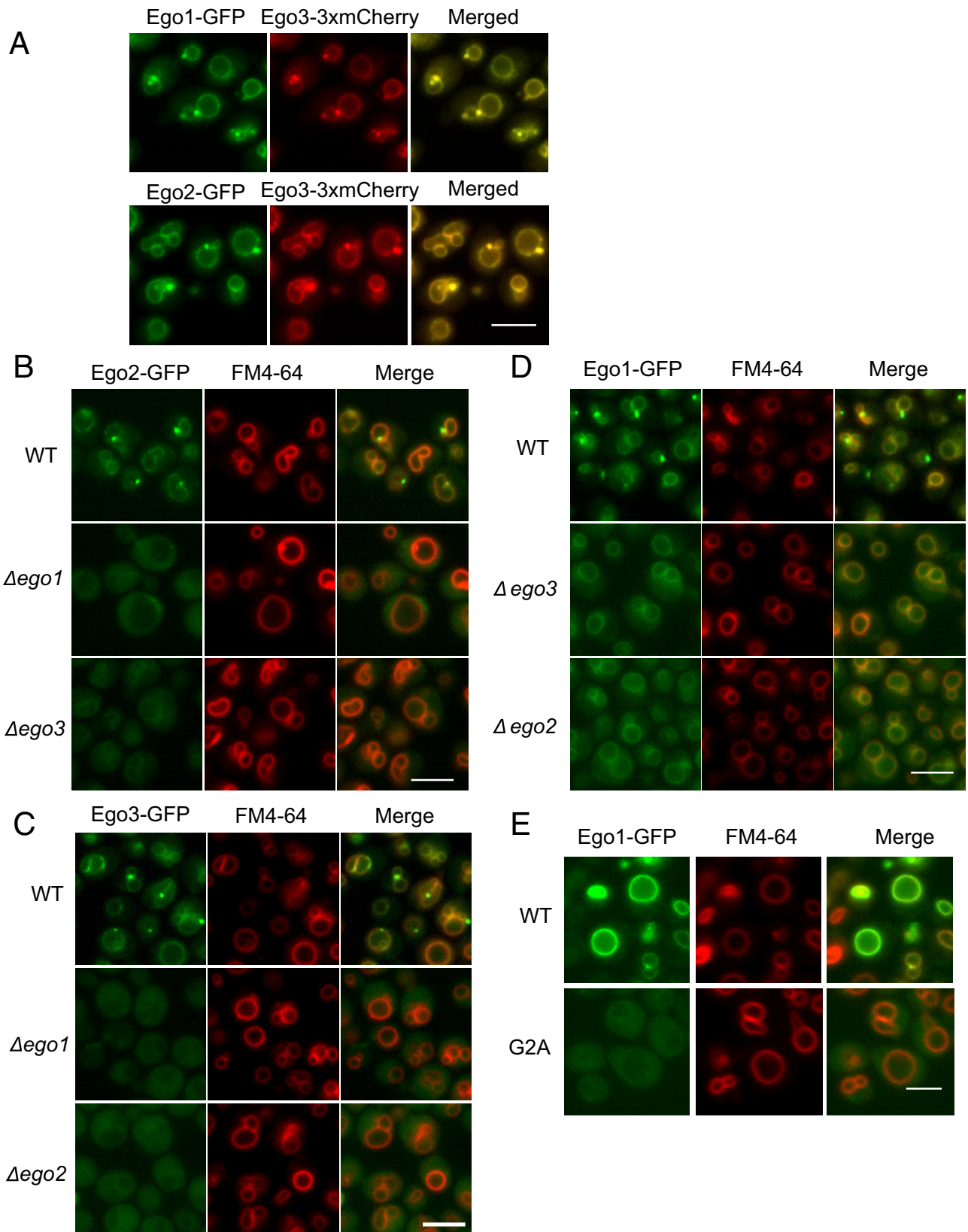


FIGURE 1: Ego2 is localized on the vacuole and its associated puncta, along with Ego1 and Ego3. (A) Diploid cells expressing both Ego1-GFP and Ego3-3xmCherry (YKY033-A) or Ego2-GFP and Ego3-3xmCherry (YKY037-A). (B–D) WT (SKY331-A), $\Delta ego1$ (SKY353-A), and $\Delta ego3$ (SKY354-A) cells expressing Ego2-GFP (B), WT (SKY114-A), $\Delta ego1$ (SKY115-A), and $\Delta ego2$ (SKY340-A) cells expressing Ego3-GFP (C), and WT (SKY108-A), $\Delta ego3$ (SKY326-A), and $\Delta ego2$ (SKY339-A) cells expressing Ego1-GFP (D) were stained with FM4-64. (E) $\Delta ego1$ (NKY002) cells expressing Ego1-GFP (WT [pSK384] or G2A mutant [pSK385]). Bar, 5 μ m.

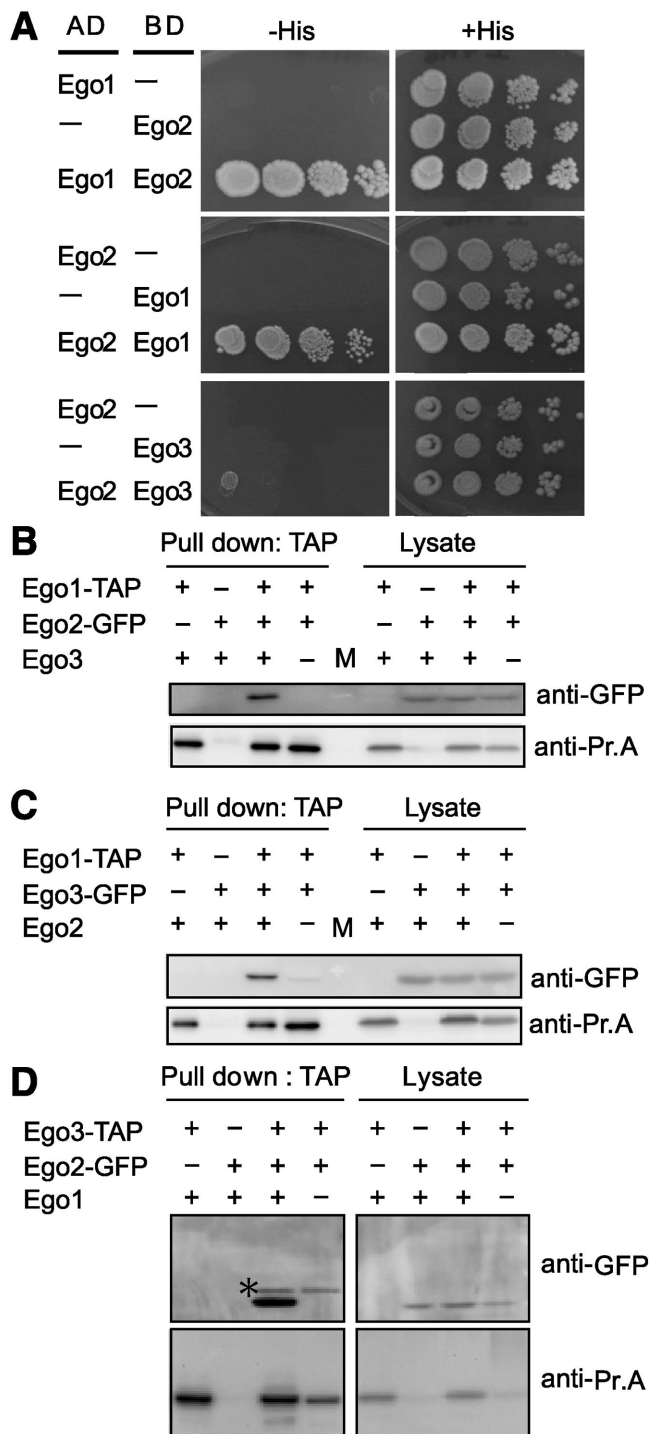


FIGURE 2: Ego2 is associated with Ego1 and Ego3. (A) Yeast two-hybrid analysis to detect interactions between Ego1 and Ego2 or Ego2 and Ego3. Strain PJ69-4A harboring pGAD-C1 and pGBD-C1, empty vectors, and pYKY8, 9, or 11–13 was serially 10-fold diluted and spotted on the indicated selective plates. (B–D) Lysate of cells expressing Ego1-TAP (B), Ego3-TAP (C), or Ego2-TAP (D) were subjected to TAP pull down using immunoglobulin G–Sepharose and Western blotting. Strains used were SKY331-A, SKY256-A, YKY030-A, and SKY469-A (B); SKY256-A, SKY114-A, YKY028-A, and SKY470-A (C); and SKY331-A, YKY024-A, YKY031-A, and YKY131 (D).

Ego2 is partially involved in anchoring Gtr complex on vacuole

Ego1 forms a complex with Gtr1 and Gtr2 (Gao and Kaiser, 2006), and we showed that Ego1-GFP colocalized with Gtr1-3xmCherry (Figure 4A). Consistent with the foregoing model, in which Ego2 is a subunit of Ego, Ego2-GFP also colocalized with Gtr1-3xmCherry (Figure 4A). We previously demonstrated that GFP-Tor1, replacing the endogenous TOR1 gene and driven by its own promoter, complemented Tor1 function (Kira *et al.*, 2014). Here we showed that Ego3-3xmCherry colocalized with GFP-Tor1 (Figure 4B). We also determined the localization of another TORC1 subunit, Tco89 (Reinke *et al.*, 2004). N-terminally GFP-tagged Tco89 driven by its own promoter complemented the protein's native function, as determined by rapamycin-sensitivity assay (Supplemental Figure S3A). Like GFP-Tor1, GFP-Tco89 colocalized with Ego3-3xmCherry (Supplemental Figure S3B), indicating that these signals mostly represent the localization of TORC1. Therefore TORC1 proteins colocalize on the vacuole and the puncta with Ego1/2/3 Gtr1.

In $\Delta ego1$ and $\Delta ego3$ mutants, localization of Gtr GTPases on the vacuole is lost (Figure 4, C and D; Dubouloz *et al.*, 2005). By contrast, although vacuolar localization of Gtr1 was also significantly reduced in the $\Delta ego2$ mutant, a limited amount of Gtr1-GFP signal remained on the vacuole (Figure 4C). This remaining Gtr1 may explain the partial Gtr1-dependent TORC1 activity in the $\Delta ego2$ mutant described in the preceding section.

Gtr1 is associated with Ego1 and Ego2 via C-terminal Roadblock domain

As previously reported, an interaction between Gtr1 and Ego1 was observed by two-hybrid analysis (Figure 5A and Supplemental Figure S1A, bottom; Gao *et al.*, 2005; Binda *et al.*, 2009; Sekiguchi *et al.*, 2014). In addition, we observed a weak interaction between Gtr1 and Ego2 in both the AD and BD combinations (Figure 5A). The Gtr1 protein consists of an N-terminal GTPase domain (G domain) and a C-terminal Roadblock domain (Gong *et al.*, 2011; Jeong *et al.*, 2012), and we separately tested the interactions of both domains. We observed a weak interaction between Ego2 and the Roadblock domain (Figure 5B) but no significant interaction between Ego2 and the G domain, even if it takes GTP-bound form (Figure 5B). Similarly, Ego1 interacted with the Roadblock domain but not the G domain of Gtr1 and Ego1 (Figure 5B). Thus Ego2 and Ego1 both interact with the C-terminal Roadblock domain of Gtr1. This is consistent with the idea that Gtr1 can be anchored to Ego1 even in the absence of Ego2 but that Ego2 strengthens the interaction.

Gtr1 nucleotide-loading state affects localization of Ego/Gtr/Tor1

Next we focused on the observation that these proteins colocalized on perivacuolar puncta. Vph1, a subunit of V-ATPase and a general vacuolar membrane marker protein (Zhao *et al.*, 2013), did not show such frequent puncta pattern (as the fusion Vph1-mCherry), indicating that such localization is not a general phenomenon of vacuolar membrane proteins (Figure 6D). The puncta did not exhibit significant overlap with other vacuolar membrane–associating puncta, such as the preautophagosomal structure (indicated by the marker Apel) or late endosome (indicated by the marker Snf7; Babst *et al.*, 2002; Suzuki *et al.*, 2002; Figure 6D). We also detected GFP-Sch9, a substrate of TORC1. As reported, GFP-Sch9 was enriched on the vacuolar membrane, but no obvious puncta similar to Ego were

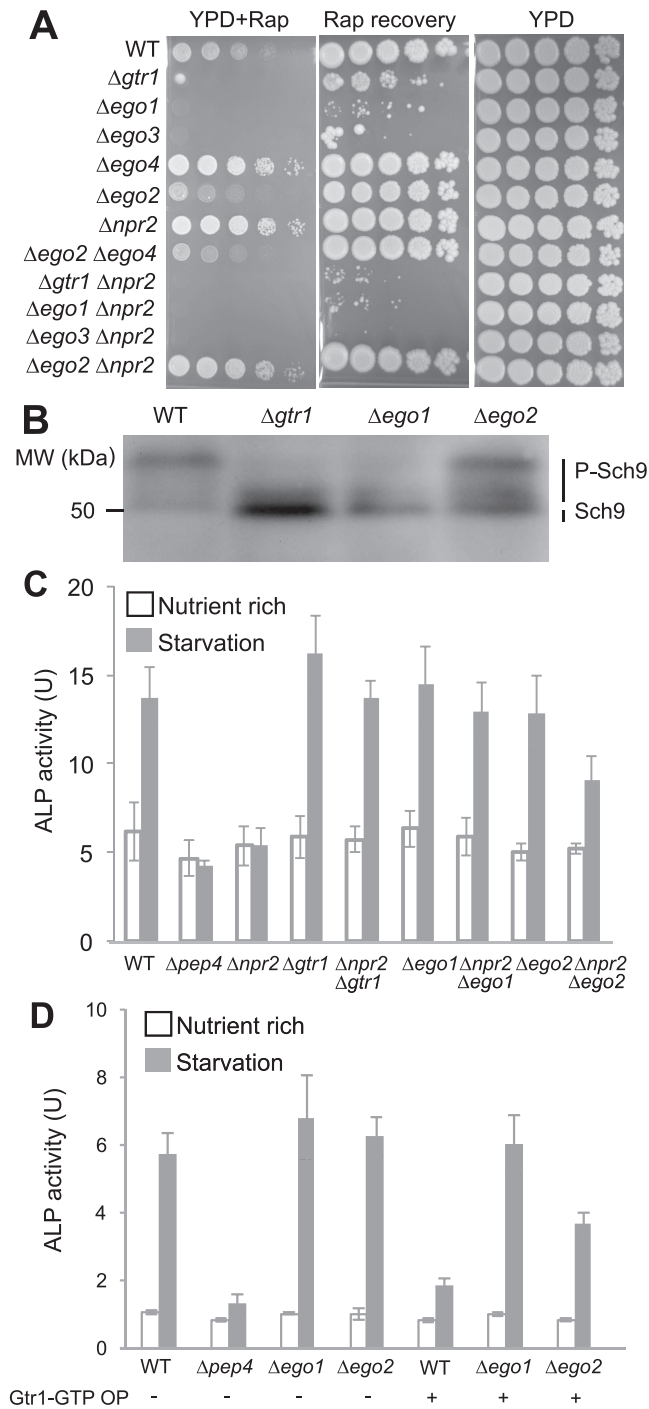


FIGURE 3: The $\Delta ego2$ mutant exhibits a partial defect in Gtr1-dependent TORC1 activation. (A) Wild-type (BY4741), $\Delta gtr1$ (NKY004), $\Delta ego1$ (NKY002), $\Delta ego3$ (NKY003), $\Delta ego4$ (YKY010), $\Delta ego2$ (YKY011), $\Delta npr2$ (SKY032-A), $\Delta ego2 \Delta ego4$ (YKY012-A), $\Delta gtr1 \Delta npr2$ (SKY037-A), $\Delta ego1 \Delta npr2$ (SKY039-A), $\Delta ego3 \Delta npr2$ (SKY040-A), and $\Delta ego2 \Delta npr2$ (SKY498-A) cells were serially 10-fold diluted and spotted onto YPD plates with or without 0.2 μ g/ml rapamycin and grown at 30°C for 3 d. The strains were also cultured for 6 h in liquid YPD containing 0.2 μ g/ml rapamycin and then grown on YPD plates at 30°C for 3 d. (B) Lysates of cells harboring Sch9-6HA in the WT (SKY116), $\Delta gtr1$ (SKY118-A), $\Delta ego1$ (SKY120-A), or $\Delta ego2$ (SKY467-A) background were treated with NTCB and subjected to Western blotting. (C) Each strain harboring Pho8 Δ 60 was grown in YPD and nitrogen starved for 4 h. Lysates were subjected to ALP assay to measure autophagic activity. Strains were as follows:

observed (Figure 6E; Urban et al., 2007; Jin et al., 2014). However, almost half of the puncta (45%) were localized at sites positive for Nup49-mCherry, a nuclear envelope marker (Stone et al., 2000; Figure 6D). The nuclear–vacuolar junction marker Vac8 also exhibited significant overlap (43%; Pan et al., 2000; Figure 6D), implying that the puncta tend to be organized at nuclear–vacuolar junctions.

This punctate localization of Ego1, Ego3, and Ego2 was mostly absent in the *GTR1* and *GTR2* deletion mutants, whereas vacuolar membrane localization persisted (Figure 6, A–C). Thus the Gtr proteins play critical roles in punctate localization. Lack of punctate localization of Ego1-GFP in the $\Delta ego3$ and $\Delta ego2$ mutants could be attributed to loss of Gtr1/2 localization in these mutants (Figure 1D). Previously, we reported that the GTP/GDP form of Gtr1 affects GFP-Tor1 localization (Kira et al., 2014). When Gtr1 is in the GTP-bound form, GFP-Tor1 preferentially localizes on the vacuole membrane (Kira et al., 2014). We also investigated whether the punctate localization of GFP-Tor1 was affected by the nucleotide-loading state of Gtr1. The Gtr1 Q65L mutant (a mimic of the GTP-bound state; Gao and Kaiser, 2006) dramatically decreased the punctate localization of GFP-Tor1, whereas the Gtr1 S20L mutant (a mimic of the GDP-bound state) increased the number of puncta (Figure 7A). We also confirmed that vacuolar localization of GFP-Tco89, like that of GFP-Tor1, was elevated in cells expressing Gtr1-GTP Gtr2-GDP (Supplemental Figure S3C; Kira et al., 2014).

The GFP-labeled GTP-bound Gtr1 mutant itself also mostly localized on the vacuolar membrane and barely localized at puncta (Figure 7B). By contrast, the GDP-bound Gtr1 mutant was exclusively found on puncta (Figure 7B). Although the GDP-bound Gtr1 mutant was unstable relative to the WT protein (Supplemental Figure S2A), the intensities of the punctate signals of the mutant protein did not decrease (Figure 7B).

Localization of Ego subunits was also affected by the nucleotide-loading state of Gtr1. In GTP-bound Gtr1 mutant cells, Ego1, Ego3, and Ego2 were exclusively localized on the vacuolar membrane, and the punctate signals were mostly absent (Figure 7, C–E). On the contrary, the number of cells containing Ego puncta were elevated in GDP-bound Gtr1 mutant cells, in which the signals on the vacuolar membrane were greatly reduced (Figure 7, C–E), although the expression levels of Ego1/3/4-GFP were not affected in these mutants (Supplemental Figure S2, B–D). Taking the results together, we concluded that the Gtr1 nucleotide-bound state affects localization of Ego/Gtr/TORC1.

Gtr2 actively localizes TORC1 on perivacuolar foci

We previously reported that GFP-Tor1 is localized primarily on puncta in the $\Delta gtr1 \Delta gtr2$ double mutant (Kira et al., 2014), suggesting that puncta are the default destination of TORC1 in the absence of Gtr proteins. Gtr1 lacking only the G domain (Gtr1 Δ G) was able to localize on the vacuolar membrane (Figure 8A), but GFP-Tor1 was mostly mislocalized on puncta (Figure 8C), supporting the suggestion that the Gtr1 G domain is required for TORC1 vacuolar localization. Consistently, Gtr1 Δ G was not able to activate TORC1, as determined by the rapamycin-sensitivity assay (Figure 8E).

WT (SKY084-A), $\Delta pep4$ (SKY100-A), $\Delta npr2$ (SKY091-A), $\Delta gtr1$ (SKY244-A), $\Delta npr2 \Delta gtr1$ (SKY245-A), $\Delta ego1$ (SKY129), $\Delta npr2 \Delta ego1$ (YKY145), $\Delta ego2$ (YKY147), $\Delta npr2 \Delta ego2$ (YKY146). (D) WT (SKY084-A), $\Delta pep4$ (SKY100-A), $\Delta ego1$ (SKY129), and $\Delta ego2$ (YKY147) cells harboring pRS316 or pSK205 (pRS316/pGal1-GST-Gtr1) were grown in SCGal medium until log phase and starved for 4 h in SD-N medium. Lysates were subjected to ALP assay.

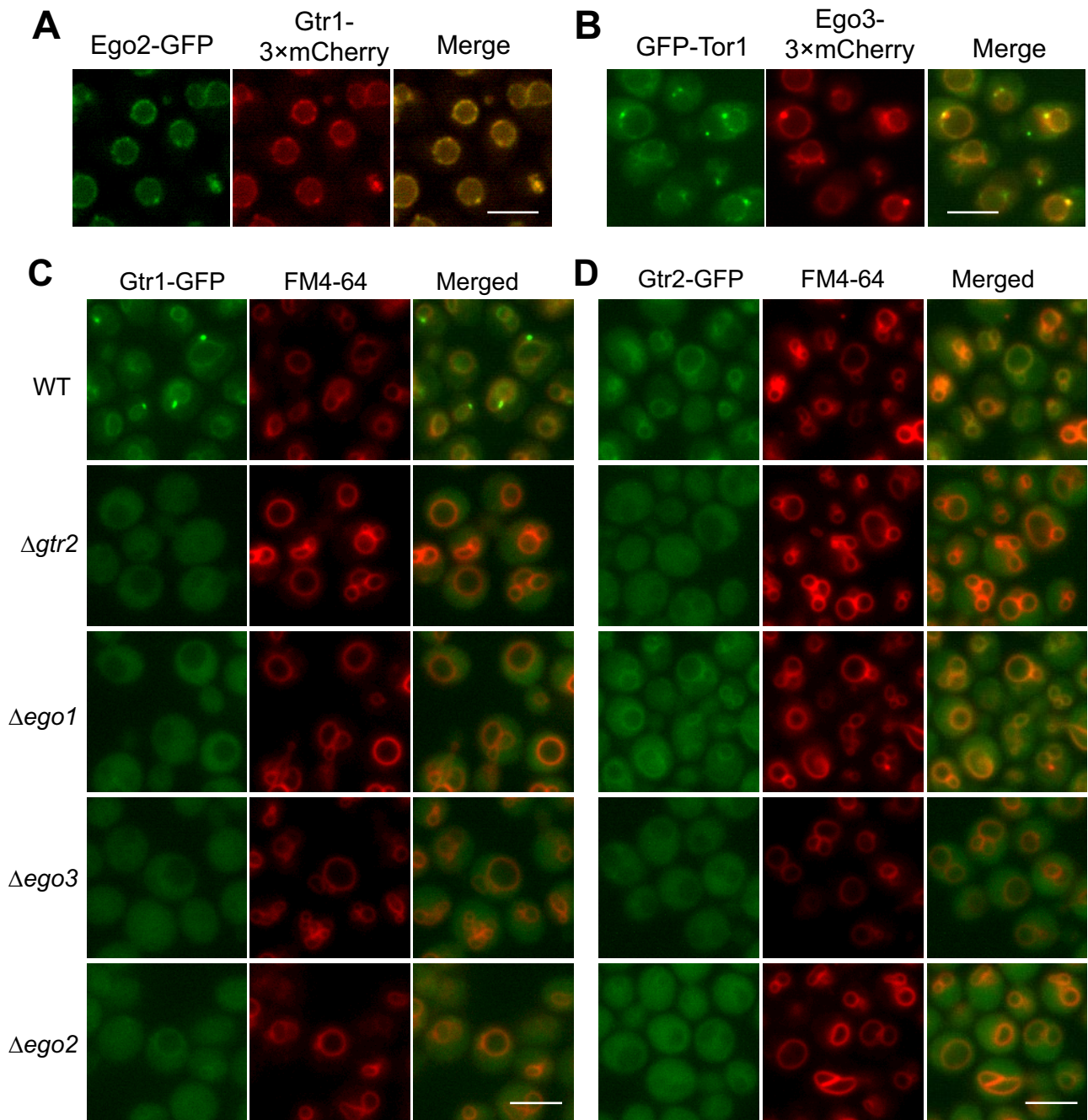


FIGURE 4: The $\Delta ego2$ mutant exhibits a partial defect in vacuolar localization of Gtr1. (A, B) Diploid cells expressing Ego2-GFP and Gtr1-3xmCherry (YKY034-A; A) or GFP-Tor1 and Ego3-3xmCherry (YKY118-A; B). (C, D) Wild-type and mutant strains expressing Gtr1-GFP or Gtr2-GFP were stained with FM4-64. (C) WT (SKY112-A), $\Delta gtr2$ (SKY249-A), $\Delta ego1$ (SKY250-A), $\Delta ego3$ (SKY113-A), $\Delta ego2$ (SKY337-A). (D) WT (SKY259-A), $\Delta gtr1$ (SKY260-A), $\Delta ego1$ (SKY261-A), $\Delta ego3$ (SKY323-A), $\Delta ego2$ (SKY338-A). Bar, 5 μ m.

When Gtr2 is deleted, Gtr1 cannot be localized on the vacuole, suggesting that Gtr1/Gtr2 heterodimer formation stabilizes the protein's normal localization (Kira *et al.*, 2014). We found that Gtr2 lacking only the G domain (Gtr2 Δ G) could be localized on the vacuolar membrane in a Gtr1-dependent manner (Figure 8B) and to maintain Gtr1-GFP localization on the vacuole (Figure 9A). However, GFP-Tor1 was mislocalized on puncta in the Gtr2 Δ G mutant (Figure 8D). Therefore Gtr1-dependent localization of TORC1 is defective in Gtr2 lacking the G domain, even though Gtr1 is localized on the vacuole. Furthermore, Gtr2 Δ G did not complement the rapamycin sensitivity

of $\Delta gtr2$ cells (Figure 8E). Autophagy was suppressed by expression of Gtr1-GTP in Gtr2-GDP cells but not in the Gtr2 Δ G mutant (Figure 8F). Therefore Gtr1-dependent activation of TORC1 is also defective in Gtr2-expressing cells that lack the G domain.

When the Gtr2 G domain was deleted, localization on Gtr1-GFP puncta was still mostly absent, indicating that the Gtr2 G domain is also important for formation of Gtr1-GFP puncta (Figure 9A), although both the GTP and GDP forms of Gtr2 mutants maintain GFP-Gtr1 puncta formation (Figure 9B). Therefore the Gtr2 G domain determines Gtr1 localization independent of its nucleotide-bound form.

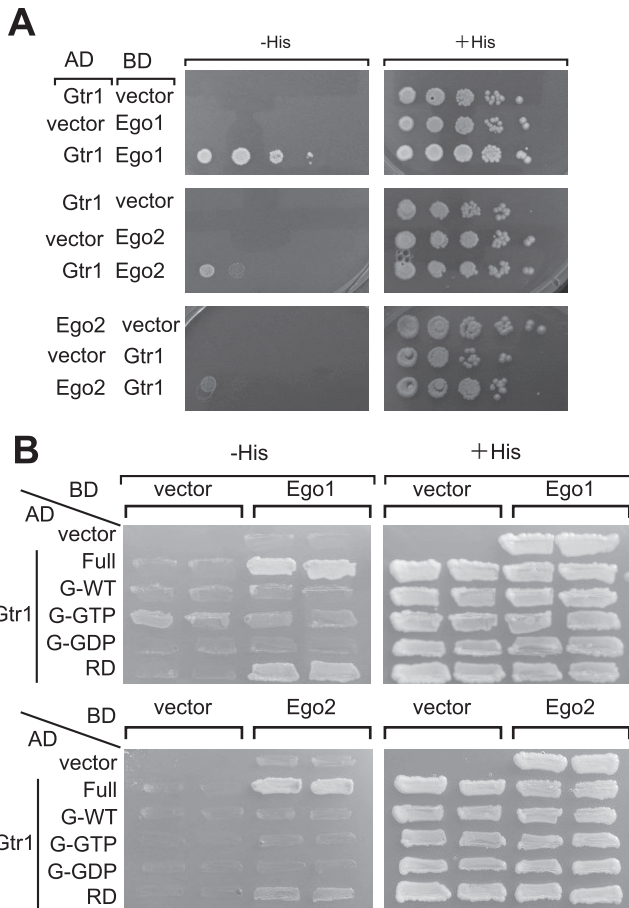


FIGURE 5: Ego1 and Ego2 interact with the Gtr1 Roadblock domain. (A) PJ69-4A cells harboring the indicated plasmids (pGAD-C1 and pGBD-C1, and pYKY009, 012, 013, pSK132, or 147) were grown on $-His$ and $+His$ plates for 6 d. (B) PJ69-4A harboring the indicated plasmids (Gtr1 G domain [WT: pSK359; Q65L: pSK360; S20L: pSK361] and Gtr1 Roadblock domain [pSK362], Ego1 [pYKY024], and Ego2 [pYKY026]) were grown on SD medium with or without histidine.

We next investigated whether Gtr2 participates actively in TORC1 localization on puncta. We reported previously that Gtr2 binds directly to the TORC1 subunit Kog1, and this interaction is involved in suppressing TORC1 activity when Gtr1 is in the GDP-bound form (Kira *et al.*, 2014). A Gtr2 allele with a point mutation at the probable Kog1-binding surface (E62K) loses its Kog1-binding capacity and TORC1 suppression activity (Kira *et al.*, 2014). However, even in the $\Delta gtr1\Delta gtr2$ double mutant expressing Gtr1 (GDP) Gtr2 (E62K), GFP-Tor1 formed puncta to approximately the same degree as in the Gtr1 (GDP) mutant (Supplemental Figure S3D). However, as just detailed, GFP-Tor1 is also localized on puncta in the absence of Gtr proteins, and we were not able to determine whether loss of TORC1 association in the Gtr1 (GDP) Gtr2 (E62K) mutant leads to GFP-Tor1 puncta mislocalization.

To investigate the foregoing possibility, we artificially targeted GFP-Tor1 to the vacuolar membrane by achieving expression of GFP-binding protein (GBP; Kubala *et al.*, 2010) on the vacuolar membrane. To achieve this, we linked GBP to the cytoplasmic region of the vacuolar-resident, single-transmembrane protein alkaline phosphatase (Pho8), which lacks the catalytic center (i.e., amino acids 120–128 are absent). In a control experiment, this GBP-Pho8 chimeric protein was successfully shown to target GFP-Atg8 protein

(which otherwise does not localize on the vacuole; Suzuki *et al.*, 2001) on the vacuolar membrane (Supplemental Figure S4, A and B). Similarly, expression of GBP-Pho8 recovered vacuolar membrane localization of GFP-Tor1 in $\Delta gtr1\Delta gtr2$ cells, so that the percentage of such cells (35.4%) is similar to the levels of WT Gtr1/2 expression (35.9%; Supplemental Figure S4C). In particular, quantitative line-plot analysis showed that Gtr1-GDP Gtr2-GTP cells expressing GBP-Pho8 had a weaker GFP-Tor1 signal on the vacuolar membrane than $\Delta gtr1\Delta gtr2$ cells (Figure 10, A and B). On the other hand, both the Gtr2 Δ G and Gtr2 (E62K) mutants expressing GBP-Pho8 had GFP-Tor1 signal intensities on the vacuolar membrane similar to that of the $\Delta gtr1\Delta gtr2$ mutant (Figure 10, A and B). These findings show that the Gtr2 G domain actively facilitates perivacuolar foci localization of TORC1 by means of direct binding to Kog1.

Taken together, these data show that the localization of TORC1/Gtr/Ego on puncta is regulated by the nucleotide-loading state of Gtr1 and Gtr2. It is therefore expected that, when Gtr1 activates and Gtr2 inactivates TORC1, the localization of TORC1/Gtr/Ego will be shifted dynamically between the vacuolar membrane and the puncta.

DISCUSSION

Our findings in this study, together with those of a recent report (Powis *et al.*, 2015), show that Ycr075w-a is a novel subunit of the yeast Ego; accordingly, it has been named Ego2. Thus yeast Ego consists of at least four subunits: one molecule of Ego1, two of Ego3, and one of Ego2. By contrast, mammalian Ragulator consists of five subunits (p18/Lamtor1, p14/Lamtor2, MP1/Lamtor3, C7orf59/Lamtor4, and HBXIP/Lamtor5). Therefore it is reasonable to speculate that yeast Ego contains one more subunit; this notion is supported by the observation that most Roadblock proteins, including Ego2, exhibit a dimeric organization (Levine *et al.*, 2013). One potential additional subunit is Ynr034w-a/ego4, considered as a candidate based on its secondary structure (Levine *et al.*, 2013), and another possibility is that two molecules of Ego2 proteins are present (as in the case of Ego3; Zhang *et al.*, 2012). Despite several attempts (Supplemental Figure S1A; unpublished data), no positive data supporting these hypotheses are available. Powis *et al.* (2015) reported a crystal structure of Ego2 in complex with Ego3. In any case, identification of Ego2 has prompted us to discuss the overall structural relationship between yeast Ego and mammalian Ragulator.

Unexpectedly, despite the clear association of Ego2 with Ego (Figures 1 and 2), the $\Delta ego2$ mutant caused only a partial defect in Gtr1-dependent TORC1 activation, in contrast to the phenotypes of the $\Delta ego1$ and $\Delta ego3$ mutants (Figure 3); this fact was not mentioned in Powis *et al.* (2015). The difference between $\Delta ego1/\Delta ego3$ and $\Delta ego2$ could be attributed to the different efficiencies of Gtr1 association with the vacuole in each mutant: in $\Delta ego2$, the Gtr1-GFP signal on the vacuole was dramatically reduced but persisted to some extent, whereas in $\Delta ego1$, the signal was completely eliminated (Figure 4). Because Gtr1 directly binds to Ego1 via its Roadblock domain (Figure 5B), at least a small fraction of Gtr1 can be anchored to the vacuole via Ego1 even in the absence of Ego2, and this might be sufficient for partial TORC1 activation. Ego2 may facilitate this binding via direct interaction with Gtr1 (Figure 5A) and/or stabilization of the association between Ego3 and Ego1 (Figures 1 and 2). Meanwhile, it is intriguing that the $ego3$ mutant exhibited the same degree of rapamycin sensitivity as the $ego1$ mutant (Figure 3A). Ego3 seems to play a more critical role in Gtr1-dependent TORC1 activation than Ego2 (Figure 3), although no direct interaction between Ego3 and Gtr1 could be detected by two-hybrid analysis (Supplemental Figure S1A). However, the $\Delta ego2$ mutant

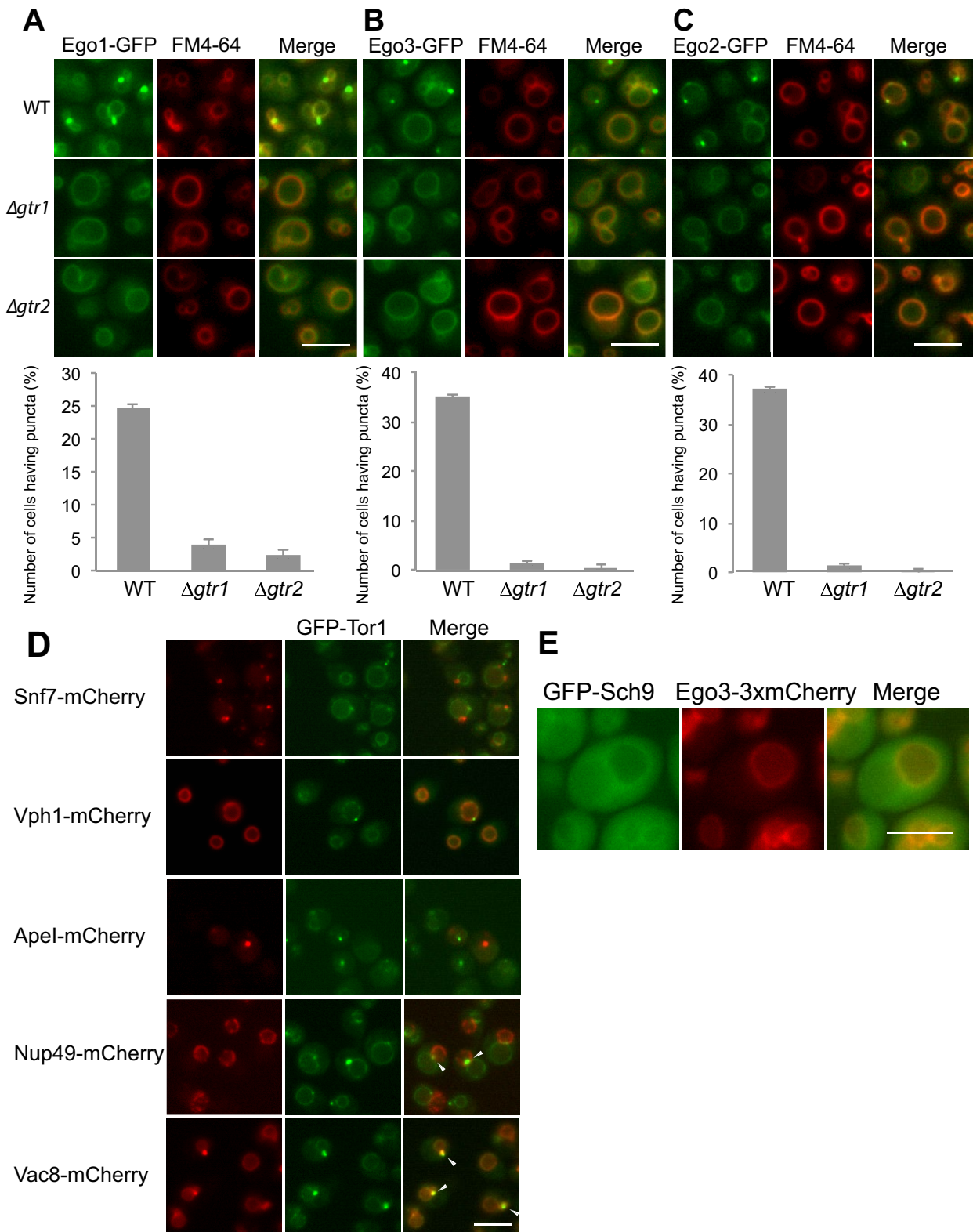


FIGURE 6: Localization of Ego proteins in Δgtr mutants and the relationship with the other markers. (A–C) Wild-type, $\Delta gtr1$, and $\Delta gtr2$ cells expressing (A) Ego1-GFP, (B) Ego3-GFP, and (C) Ego2-GFP. The mean and standard deviation of percentages of cells having GFP puncta from three independent experiments (200–300 cells each) are shown. Strains were as follows: Ego1-GFP (WT: SKY108-A; $\Delta gtr1$: SKY262-A; $\Delta gtr2$: SKY263-A), Ego3-GFP (WT: SKY114-A; $\Delta gtr1$: SKY327-A; $\Delta gtr2$: SKY361-A), and Ego2-GFP (WT: SKY331-A; $\Delta gtr1$: SKY351-A; $\Delta gtr2$: SKY352-A). (D) Cells expressing GFP-Tor1 and C-terminally mCherry-tagged Snf7 (SKY236-A), Vph1 (SKY461-A), Apel (SKY395-A), Nup49 (SKY374-A), or Vac8 (SKY451-A). Arrowheads indicate GFP-Tor1 punctate structure adjacent to Nup49-labeled nuclear envelope, and GFP-Tor1 dots colocalized with the Vac8 perivacuolar dot structure. Bar, 5 μ m. (E) Cells expressing pNop1-GFP-Sch9 and Ego3-3xmCherry (SKY519). Bar, 5 μ m.

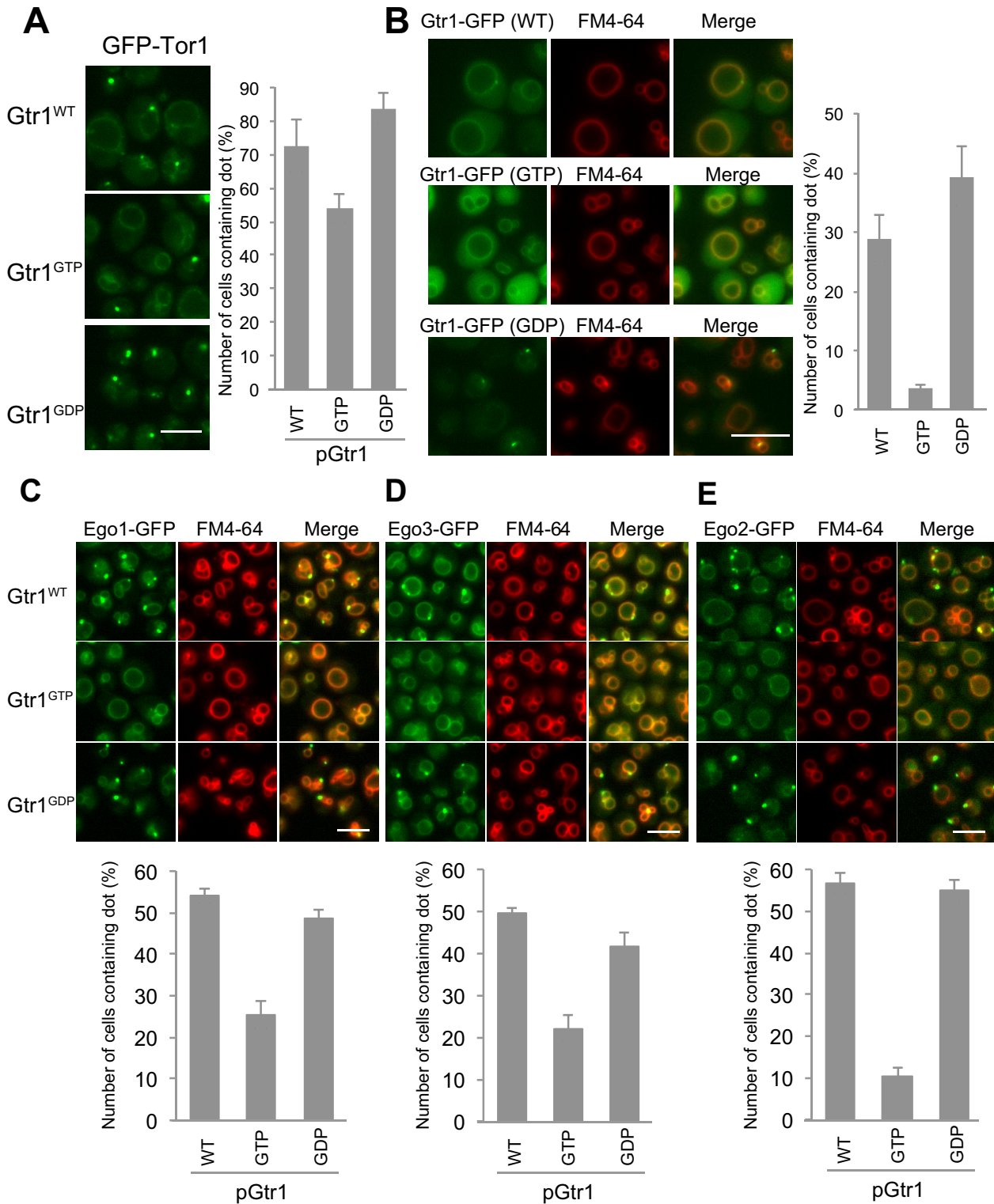


FIGURE 7: Tor1 and Ego protein localization in Gtr1 nucleotide-loading-state mutant. (A) GFP-Tor1 $\Delta gtr1$ (SKY278-A) cells harboring pRS316 or Gtr1 (WT: pSK114; Q65L[GTP]: pSK116; and S20L[GDP]: pSK115 mutant). Bar, 5 μ m. (B) $\Delta gtr1$ cells (NKY004) harboring single-copy plasmid expressing Gtr1-GFP (WT: pSK274; Q65L[GTP]: pSK277; and S20L[GDP]: pSK286 mutant) were subjected to microscopy. (C–E) $\Delta gtr1$ cells expressing (C) Ego1-GFP (SKY262-A), (D) Ego3-GFP (SKY327-A), or (E) Ego2-GFP (SKY351-A) and harboring a plasmid encoding Gtr1 (WT: pSK114; Q65L[GTP]: pSK116; and S20L[GDP]: pSK115 mutant). Bar, 5 μ m. The mean and standard deviation of percentages of cells having GFP puncta from three independent experiments (200–300 cells each) are shown.

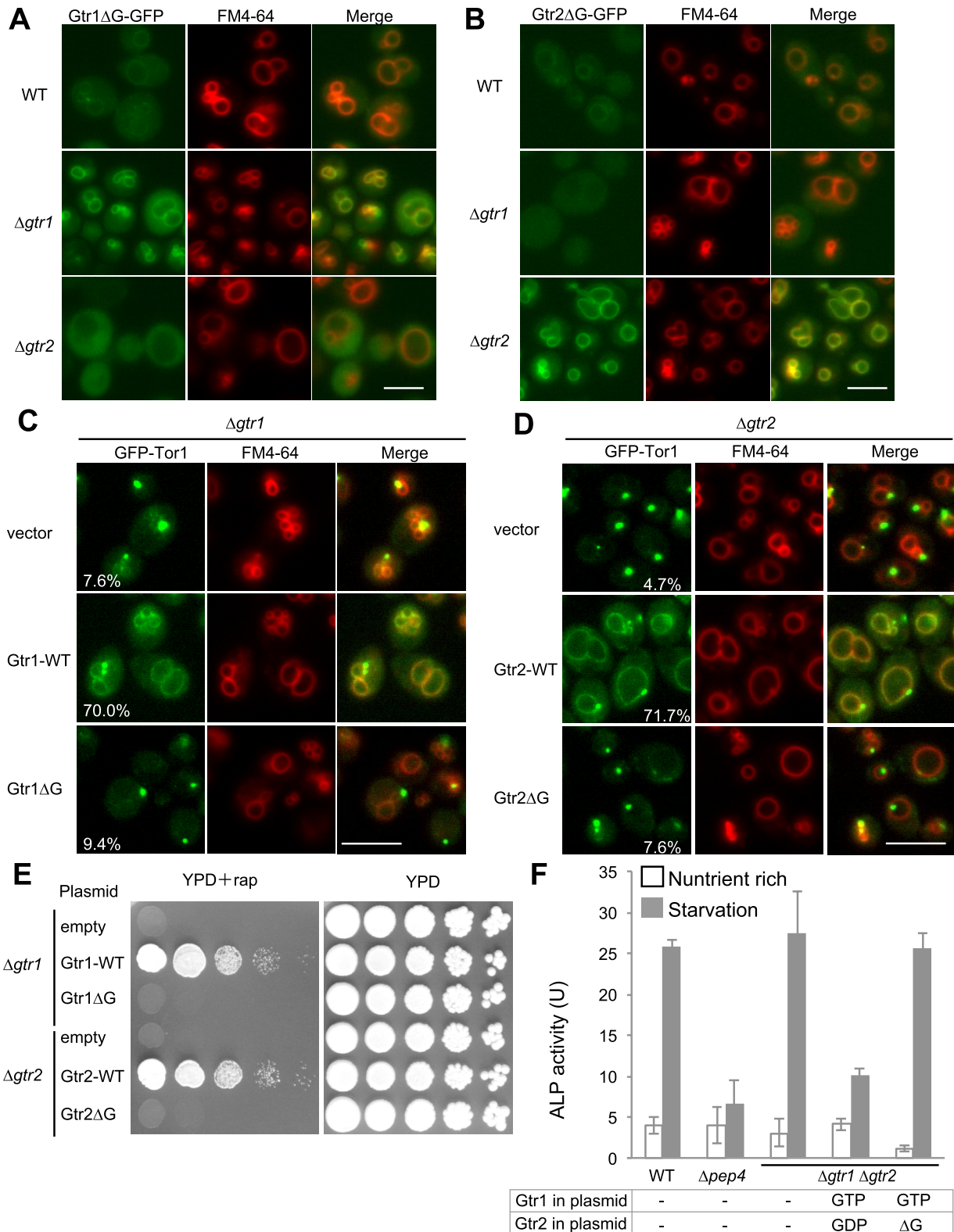


FIGURE 8: Gtr2 G domain is required for Gtr1-dependent TORC1 activation. (A, B) WT, Δ *gtr1*, and Δ *gtr2* (KNY 004, KNY 005) harboring (A) pRS316/Gtr1 Δ G-GFP and (B) pRS316/Gtr2 Δ G-GFP. (C, D) GFP-Tor1 in Δ *gtr1* or Δ *gtr2* (SKY278-A, SKY279-A) harboring Gtr1,2-WT (pSK114, pSK100) or Gtr1,2 Δ G (pSK291, pSK293). Percentage of cells in which GFP-Tor1 is detected over the vacuolar membrane is shown for each image. The average of three independent experiments (200–300 cells each) is shown. (E) Δ *gtr1* or Δ *gtr2* (EUROSCARF) harboring empty vector (pRS316), pSK114, pSK291, pSK100, or pSK293 was serially 10-fold diluted and spotted on YPD plates with or without 0.2 μ g/ml rapamycin and grown at 30°C for 3 d. (F) WT (SKY084-A) or Δ *pep4* (SKY100-A) harboring empty vector and Δ *gtr1* Δ *gtr2* harboring empty vector, Gtr1-GTP Gtr2-GDP (pSK129), or Gtr1-GTP Gtr2 Δ G (pSK345), cultured logarithmically in SCD or starved for 4 h in SD-N medium, were subjected to ALP assay.

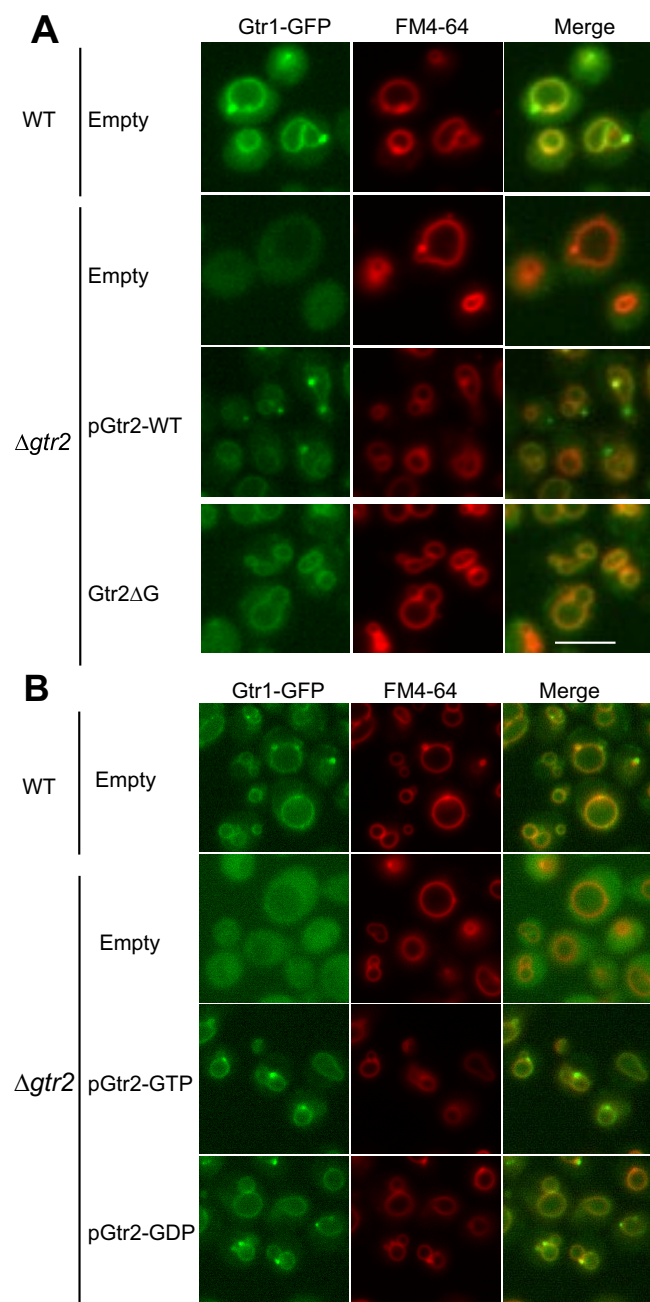


FIGURE 9: Gtr2 affects Gtr1 and Tor1 perivacuolar localization. (A, B) Localization of Gtr1-GFP in various Gtr2 mutants, determined by microscopy. Gtr1-GFP WT (SKY112-A) and $\Delta gtr2$ (SKY249-A), harboring a plasmid expressing Gtr2 WT (pSK100) and Gtr2- ΔG (pSK293; A), and a Gtr2-GTP mutant (pSK93) and Gtr2-GDP mutant (pSK92; B).

also had a defect in Ego3 localization (Figure 1C). These observations might be reconciled if a very low level (not detectable using our microscope system) of Ego3 remains on the vacuole in the $\Delta ego2$ mutant. This possibility is consistent with the observation that Ego2-GFP is slightly detectable on the vacuole even in $\Delta ego3$ mutant cells (Figure 1B). In any case, Ego3 seems to exert a greater effect on Gtr1 than does Ego2. In mammals, Ragulator has been proposed to play a role not only as a scaffold but also as a guanine nucleotide exchange factor (GEF) for RagA/B, which corresponds to Gtr1 (Bar-Peled *et al.*, 2012). It is reasonable to hypothesize that

Ego also possesses such a function, and these observations support further investigations of that possibility. Powis *et al.* (2015), however, showed that artificial targeting of Gtr1/Gtr2 in $\Delta ego1\Delta ego2\Delta ego3$ cells can activate TORC1, indicating that Gtr1 can bypass all functions of Ego other than its role as a scaffold. Vam6/Vps39 may serve as the GEF for Gtr1, at least in yeast (Binda *et al.*, 2009).

By analyzing the detailed localization of Ego2, we showed for the first time that Ego1, 3, and 2, Gtr1 and 2, and TORC1 are colocalized on the vacuole and its associated puncta (Figure 4, A and B). In particular, puncta localization should be of interest because the accumulation at puncta seems to be an active process directed by Gtr1 and nucleotide-loading status (Figure 7). Because Ego1 is anchored to the vacuolar membrane via its N-terminal lipid modification (Figure 1E), the puncta are likely to represent the accumulation of these proteins on the vacuolar surface rather than a structure that is detached from the vacuole. This accumulation tends to form at nuclear–vacuolar junctions (Figure 6D), possibly because the proteins maybe trapped by a physical barrier generated by contact between two bulky organelles. Recent work showed that the I-BAR protein Iy1, which plays a role in vacuolar morphology, is also colocalized with Gtr and Ego on the vacuole and puncta, and it also colocalizes with Ypt7 (Numrich *et al.*, 2015). Therefore these puncta may be important for vacuolar morphology. The GTP form of Gtr1 seems to be necessary for localization of TORC1 on the vacuolar membrane; without it, TORC1 tends to accumulate at the puncta (Figure 8C and Supplemental Figure S3C; Kira *et al.*, 2014), suggesting that the puncta are the default destination. However, our results argue against such a simple interpretation. The efficiency of GFP-Tor1 targeting to the vacuolar membrane, using an artificial method based on the affinity between GFP and GBP, was higher in a mutant lacking Gtr1 and Gtr2 than in the Gtr1-GDP and Gtr2-GTP mutants (Figure 10). This increase was also observed in a mutant lacking the Gtr2 G domain or in cells expressing Gtr2 lacking the ability to bind TORC1 (E62K; Figure 10). These data indicate that in combination with default puncta formation, Gtr2-GTP also actively participates in recruiting TORC1 to the puncta. This is in agreement with our previous proposal that Gtr2 functions directly in the inactivation of TORC1 (Kira *et al.*, 2014). Thus Gtr1 and Gtr2 play a tug of war, pulling TORC1 between the vacuolar membrane and puncta according to their nucleotide-loading status.

Activation of TORC1 by the GTP form of Gtr1 promotes vacuolar membrane localization (Figure 7A). Moreover, in contrast to $\Delta ego1$ and $\Delta ego3$, in the $\Delta ego2$ mutant, Gtr1 was still partially localized to the vacuolar membrane, and partial Gtr1-dependent TORC1 activity persisted (Figures 3 and 4C). In the mammalian system, mTORC1 is activated by recruitment to the lysosome via the Rag complex and resulting encounter with the activator Rheb GTPase (Sancak *et al.*, 2010). However, in the yeast system, it is unclear how activation is achieved and whether the Rheb homologue is involved (Urano *et al.*, 2000). It is an open question whether this dynamic relocation is associated with the regulation of TORC1 activity. If a hypothetical TORC1-activating molecule (corresponding to mammalian Rheb) is scattered over the vacuolar membrane, this relocation could lead to the regulation of TORC1 activity. Alternatively, a more plausible role for this dynamic relocation is that it would make TORC1 protein kinase more easily accessible to its substrates by dispersing it throughout the vacuolar membrane rather than allowing it to remain concentrated on the puncta. For example, Sch9, a TORC1 substrate protein, is enriched on the vacuolar membrane (Figure 6E; Urban *et al.*, 2007; Jin *et al.*, 2014). Another soluble substrate, Atg13, is localized on the vacuole-associated preautophagosomal structure (PAS) when it is dephosphorylated under starvation conditions

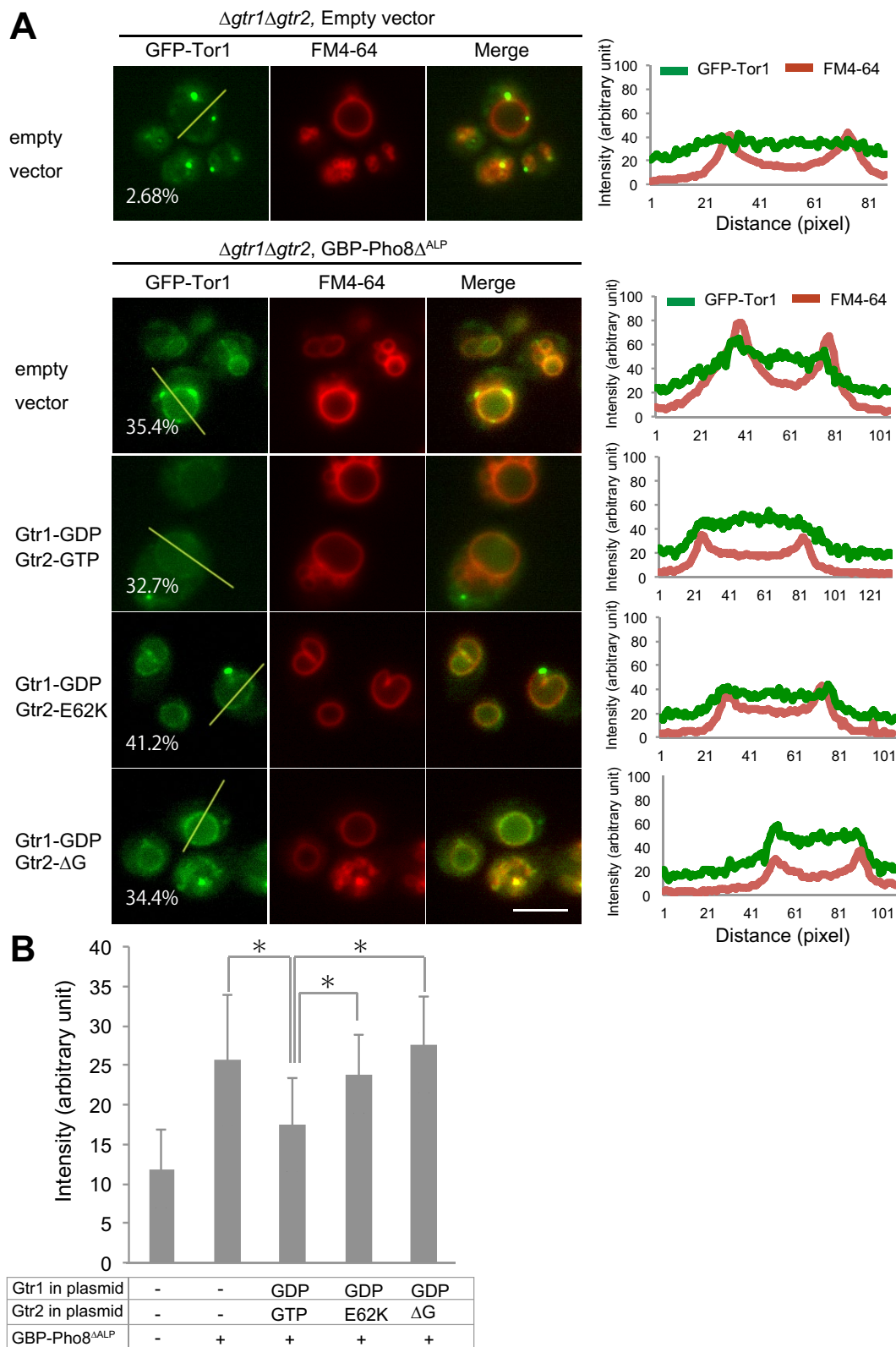


FIGURE 10: Gtr2 actively participate in the formation of the puncta of TORC1. (A) GFP-Tor1 $\Delta gtr1\Delta gtr2$ (SKY50-A) cells harboring both pRS314 (empty or pRS314/pADH1-GBP-Pho8 $\Delta^{120-128}$ [pSK413]) and pRS316 (empty, pRS316/Gtr1-GDP Gtr2-GTP [pSK127], pRS316/ Gtr1-GDP Gtr2-E62K [pSK256], or pRS316/Gtr1-GDP Gtr2- Δ G [pSK344]) series vectors were stained with FM4-64. Percentages of cells showing GFP-Tor1 localization on vacuolar membrane are shown for each image; average of three independent experiments (200–250 cells each). Right, signal intensities of GFP-Tor1 and FM4-64 along the indicated lines measured by ImageJ software (see *Materials and Methods*). (B) Signal intensities of GFP-Tor1 on the vacuolar membrane measured in A. Average and SD of the intensities from 40 points. Pixel size, 0.07 μ m. * $p < 0.01$ (t test).

(Suzuki *et al.*, 2001; Kawamata *et al.*, 2008). On addition of nutrients, Atg13 is rapidly phosphorylated by TORC1 (Kamada *et al.*, 2000). Because the PAS is distinct from the Gtr/Ego/Tor1 puncta, although it is associated with the vacuolar membrane (Figure 6D), TORC1 would be unable to encounter Atg13 until it is disseminated throughout the vacuolar membrane. However, one observation that makes interpretation more difficult is that simply shifting cells from nutrient-rich to nitrogen-starvation conditions did not dramatically induce such relocation (Kira *et al.*, 2014). This can be reconciled by the additional observation that even in the absence of Gtr1, autophagy is induced mostly normally (Kira *et al.*, 2014), implying the existence of a Gtr1-independent TORC1 activation pathway (Stracka *et al.*, 2014). In addition, artificial targeting of Tor1 onto the vacuolar membrane could not fulfill the function of Gtr1/Gtr2, at least in the experimental system we used (Figure 10, A and B, and Supplemental Figure S4D). Future studies should give a clearer view of the physiological relevance of this dramatic relocation.

By identifying Ego2 as an additional subunit of yeast Ego, this study provides insight into the detailed mechanisms underlying the dynamics of the Ego/Gtr/TORC1 proteins. Our findings should help to fundamentally elucidate the regulation of TORC1 by nutrient availability.

MATERIALS AND METHODS

Yeast strains, media, and plasmid construction

Yeast strains used in this study, most of them BY4741/4742 background (Brachman *et al.*, 1998), are listed in Supplemental Table S1. Yeast cells were grown in YPD (1% yeast extract [BD Biosciences, San Jose, CA]; 2% peptone [BD Biosciences; 2% glucose [Wako, Osaka, Japan]) or SCD (0.17% yeast nitrogen base without amino acids and ammonium sulfate [BD Biosciences], 0.5% (NH₄)₂SO₄ [Nacalai Tesque, Kyoto, Japan], 0.5% casamino acid [BD Biosciences], 2% glucose), or SCG (0.17% yeast nitrogen base without amino acids and ammonium sulfate [BD Biosciences], 0.5% (NH₄)₂SO₄ [Nacalai Tesque], 0.5% casamino acid [BD Biosciences], 2% galactose). Strain construction, gene deletion, and chromosomal epitope tagging were performed as previously reported (Longtine *et al.*, 1998; Janke *et al.*, 2004; Khmelinskii *et al.*, 2011; Nakatogawa *et al.*, 2012). For two-hybrid analysis, to replace the *LEU2* marker of pGBD-C1 with *TRP1*, a fragment containing *TRP1* was PCR amplified from pRS314, digested with *PvuII* and *Clal*, and cloned into pGBD-C1, which was digested with *PvuII* and *Clal* to remove the region containing *LEU2*. The resultant plasmid was named pSK272. *GTR1* (full-length, G domain [amino acids 1–184], Roadblock [RD] domain [amino acids 185–310]), *EGO1*, *EGO3*, *EGO2*, and *YNR034W-A* were PCR amplified from genomic DNA and cloned into pGAD-C1, pGBD-C1, and pSK272 (James *et al.*, 1996; Supplemental Table S2). *GTR1-GFP* and *EGO1-GFP* fragments, including their promoters (818 and 822 base pairs) and terminators (583 and 516 base pairs) were amplified from the respective genomically tagged strains (Supplemental Table S1), digested with *SacI/XbaI* and *SacI/KpnI*, and cloned into pRS316 (Sikorski and Hieter, 1989). Point mutations (*GTR1* [S20L, Q65L], *EGO1* [G2A]) were introduced by two-step PCR to generate pSK277, pSK286, and pSK385, respectively. The proGal1-GST-Gtr1-termGtr1 cassette was amplified from a genomically tagged yeast strain (Longtine *et al.*, 1998) and cloned into the *XbaI/SacI* sites of pRS316, and then Q65L point mutation was introduced to generate pSK196. The C-terminal RD domains of Gtr1 and Gtr2 (amino acids 185–311 and 185–341, respectively), under the control of their own promoters (1000 base pairs) and terminators (500 base pairs), were digested with *SacI/XbaI* or *BamHI/XhoI* and cloned into pRS316 to generate

pSK291 and pSK293, respectively. The RD domains of Gtr1 and Gtr2 fused with GFP, connected to their own promoters and terminators by PCR, were digested with *SacI/XbaI* or *KpnI/XhoI* and cloned into pRS316 to generate pSK290 and pSK294, respectively. GBP-Pho8 was constructed as follows: 1000 base pairs of proADH1 was amplified by PCR and cloned into the *BamHI/EcoRI* sites of pRS314 to generate pSK409. GBP amplified from pGEX-6P/GST-GFP-nanobody (Kato *et al.*, 2015) and Pho8 open reading frame lacking its alkaline phosphatase activation center (amino acids 120–128) were fused by PCR and cloned into the *EcoRI/KpnI* sites of pSK409 to generate pSK413.

Microscopy

Cells grown in SCD were collected with centrifugation (600 × g, 2 min) and subjected to microscopy. For FM4-64 staining, cells were pelleted and resuspended in 100 μl of culture medium containing 1 μl of 1.64 mM FM4-64, incubated for 30 min, washed twice with 1 ml SCD medium, incubated for 1 h, and then subjected to microscopy. Yeast cells were observed on a Leica AF6500 fluorescence imaging system (Leica Microsystems) mounted on a DIM6000 B microscope (HCX PL APO 63.6/1.40–0.60 oil-immersion objective lens, xenon lamp; Leica Microsystems, Wetzlar, Germany) under the control of the LAS-AF software (Leica Microsystems). Line-plot analysis of GFP signal intensities was conducted with ImageJ software (National Institutes of Health, Bethesda, MD) by the following procedure: designated lines were set across single vacuole, avoiding perivacuolar puncta. The intensity of GFP at a pixel corresponding to FM4-64 peak signal intensities was subtracted from intensities of the background region over ≥10 pixels.

TAP pull-down assay

TAP pull-down assays were performed as previously reported (Kira *et al.*, 2014).

NTCB treatment for Sch9

NTCB treatments were performed as previously reported, with slight modifications (Urban *et al.*, 2007). Briefly, 10 OD units of cells were treated with 6% trichloroacetic acid for 10 min on ice, washed twice with ice-cold acetone, and dried using a SpeedVac. The pellets were redissolved in 100 μl of urea buffer (50 mM Tris-Cl, pH 7.5, 5 mM EDTA, 6 M urea, 1% SDS, 1 mM phenylmethylsulfonyl fluoride, 1× Phos-Stop [Roche, Basel, Switzerland]) and vortexed with the same volume of 0.6-mm-diameter zirconia beads (Biomedical Science, Tokyo, Japan) for 10 min at 4°C. After centrifugation at 20,000 × g for 10 min at 4°C, the lysate were mixed with 30 μl of 1 M 2-(cyclohexylamino)ethanesulfonic acid (pH 10.5) and 20 μl of 7.5 M NTCB and incubated overnight at room temperature. Each sample was mixed with 50 μl of 4× loading buffer (800 mM Tris-Cl, pH 6.8, 6% SDS, 400 mM dithiothreitol, 8 M urea, 0.04% bromophenol blue) and subjected to SDS-PAGE and Western blot analysis.

Antibodies

Anti-protein A (P-3775; Sigma-Aldrich, St. Louis, MO), anti-GFP (11814460001; Roche), anti-PGK (459250; Thermo Fisher Scientific, Waltham, MA), and anti-hemagglutinin (HA; 16B12; Covance, Princeton, NJ) antibodies were used for Western blotting.

Yeast two-hybrid analysis

Yeast two-hybrid analysis was carried out as described previously (James *et al.*, 1996; Kira *et al.*, 2014). A final concentration of 3 mM 3-aminotriazole was added to SD plates lacking histidine and supplemented with amino acids (Sherman, 2002).

ALP assays for autophagy measurement

ALP assays for autophagy measurements were performed as previously reported (Kira *et al.*, 2014).

ACKNOWLEDGMENTS

We thank Kuninori Suzuki (University of Tokyo, Tokyo, Japan) and Yoshinori Ohsumi (Tokyo Institute of Technology, Tokyo, Japan) for gifts of plasmids. We also express our gratitude to the members of our laboratory, especially Takashi Itoh, for helpful discussions about these experiments. We appreciate the technical support from the Center for Frontier Oral Science, Graduate School of Dentistry, Osaka University. This work was supported in part by grants from the Japan Society for the Promotion of Science and the Ministry of Education, Culture, Sports, Science and Technology of Japan.

REFERENCES

- Ashrafi K, Farazi TA, Gordon JI (1998). A role for *Saccharomyces cerevisiae* fatty acid activation protein 4 in regulating protein N-myristoylation during entry into stationary phase. *J Biol Chem* 273, 25864–25874.
- Babst M, Katzmann DJ, Estepa-Sabal EJ, Meerloo T, Emr SD (2002). Ecr3-III: an endosome-associated heterooligomeric protein complex required for mvb sorting. *Dev Cell* 3, 271–282.
- Bar-Peled L, Chantranupong L, Cherniack AD, Chen WW, Ottina KA, Grabiner BC, Spear ED, Carter SL, Meyerson M, Sabatini DM (2013). A tumor suppressor complex with GAP activity for the Rag GTPases that signal amino acid sufficiency to mTORC1. *Science* 340, 1100–1106.
- Bar-Peled L, Schweitzer LD, Zoncu R, Sabatini DM (2012). Ragulator is a GEF for the Rag GTPases that signal amino acid levels to mTORC1. *Cell* 150, 1196–1208.
- Binda M, Peli-Gulli MP, Bonfils G, Panchaud N, Urban J, Sturgill TW, Loewith R, De Virgilio C (2009). The Vam6 GEF controls TORC1 by activating the EGO complex. *Mol Cell* 35, 563–573.
- Brachmann CB, Davies A, Cost GJ, Caputo E, Li J, Hieter P, Boeke JD (1998). Designer deletion strains derived from *Saccharomyces cerevisiae* S288C: a useful set of strains and plasmids for PCR-mediated gene disruption and other applications. *Yeast* 14, 115–132.
- Chantranupong L, Wolfson RL, Sabatini DM (2015). Nutrient-sensing mechanisms across evolution. *Cell* 161, 67–83.
- Dubouloz F, Deloche O, Wanke V, Cameroni E, De Virgilio C (2005). The TOR and EGO protein complexes orchestrate microautophagy in yeast. *Mol Cell* 19, 15–26.
- Efeyan A, Comb WC, Sabatini DM (2015). Nutrient-sensing mechanisms and pathways. *Nature* 517, 302–310.
- Gao M, Kaiser CA (2006). A conserved GTPase-containing complex is required for intracellular sorting of the general amino-acid permease in yeast. *Nat Cell Biol* 8, 657–667.
- Gao XD, Wang J, Keppler-Ross S, Dean N (2005). ERS1 encodes a functional homologue of the human lysosomal cystine transporter. *FEBS J* 272, 2497–2511.
- Gong R, Li L, Liu Y, Wang P, Yang H, Wang L, Cheng J, Guan KL, Xu Y (2011). Crystal structure of the Gtr1p-Gtr2p complex reveals new insights into the amino acid-induced TORC1 activation. *Genes Dev* 25, 1668–1673.
- Hara K, Yonezawa K, Weng QP, Kozlowski MT, Belham C, Avruch J (1998). Amino acid sufficiency and mTOR regulate p70 S6 kinase and eIF-4E BP1 through a common effector mechanism. *J Biol Chem* 273, 14484–14494.
- Hirose E, Nakashima N, Sekiguchi T, Nishimoto T (1998). RagA is a functional homologue of *S. cerevisiae* Gtr1p involved in the Ran/Gsp1-GTPase pathway. *J Cell Sci* 111, 11–21.
- James P, Halladay J, Craig EA (1996). Genomic libraries and a host strain designed for highly efficient two-hybrid selection in yeast. *Genetics* 144, 1425–1436.
- Janke C, Magiera MM, Rathfelder N, Taxis C, Reber S, Maekawa H, Moreno-Borchart A, Doenges G, Schwob E, Schiebel E, Knop M (2004). A versatile toolbox for PCR-based tagging of yeast genes: new fluorescent proteins, more markers and promoter substitution cassettes. *Yeast* 21, 947–962.
- Jeong J-H, Lee K-H, Kim Y-M, Kim D-H, Oh B-H, Kim Y-G (2012). Crystal structure of the Gtr1p(GTP)-Gtr2p(GDP) protein complex reveals large structural rearrangements triggered by GTP-to-GDP conversion. *J Biol Chem* 287, 29648–29653.
- Jewell JL, Russell RC, Guan K-L (2013). Amino acid signalling upstream of mTOR. *Nat Rev Mol Cell Biol* 14, 133–139.
- Jin N, Mao K, Jin Y, Tevzadze G, Kauffman EJ, Park S, Bridges D, Loewith R, Saltiel AR, Klionsky DJ, Weisman LS (2014). Roles for PI(3,5)P2 in nutrient sensing through TORC1. *Mol Biol Cell* 25, 1171–1185.
- Kamada Y, Funakoshi T, Shintani T, Nagano K, Ohsumi M, Ohsumi Y (2000). Tor-mediated induction of autophagy via an Apg1 protein kinase complex. *J Cell Biol* 150, 1507–1513.
- Katoh Y, Nozaki S, Hartanto D, Miyano R, Nakayama K (2015). Architectures of multisubunit complexes revealed by a visible immunoprecipitation assay using fluorescent fusion proteins. *J Cell Sci* 128, 2351–2362.
- Kawamata T, Kamada Y, Kabeya Y, Sekito T, Ohsumi Y (2008). Organization of the pre-autophagosomal structure responsible for autophagosome formation. *Mol Biol Cell* 19, 2039–2050.
- Khmelniskii A, Meurer M, Duishoev N, Delhomme N, Knop M (2011). Seamless gene tagging by endonuclease-driven homologous recombination. *PLoS One* 6, e23794.
- Kira S, Tabata K, Shirahama-Noda K, Nozoe A, Yoshimori T, Noda T (2014). Reciprocal conversion of Gtr1 and Gtr2 nucleotide-binding states by Npr2-Npr3 inactivates TORC1 and induces autophagy. *Autophagy* 10, 1565–1578.
- Kubala MH, Kovtun O, Alexandrov K, Collins BM (2010). Structural and thermodynamic analysis of the GFP:GFP-nanobody complex. *Protein Sci* 19, 2389–2401.
- Levine TP, Daniels RD, Wong LH, Gatta AT, Gerondopoulos A, Barr FA (2013). Discovery of new Longin and Roadblock domains that form platforms for small GTPases in Ragulator and TRAPP-II. *Small GTPases* 4, 1–8.
- Ljungdahl PO (2009). Amino-acid-induced signalling via the SPS-sensing pathway in yeast. *Biochem Soc Trans* 37, 242–247.
- Loewith R, Jacinto E, Wullschlegel S, Lorberg A, Crespo JL, Bonenfant D, Oppliger W, Jenoe P, Hall MN (2002). Two TOR complexes, only one of which is rapamycin sensitive, have distinct roles in cell growth control. *Mol Cell* 10, 457–468.
- Longtine MS, McKenzie AR, Demarini DJ, Shah NG, Wach A, Brachat A, Philippsen P, Pringle JR (1998). Additional modules for versatile and economical PCR-based gene deletion and modification in *Saccharomyces cerevisiae*. *Yeast* 14, 953–961.
- Nakatogawa H, Ishii J, Asai E, Ohsumi Y (2012). Atg4 recycles inappropriately lipidated Atg8 to promote autophagosome biogenesis. *Autophagy* 8, 177–186.
- Noda T, Klionsky DJ (2008). The quantitative Pho8Delta60 assay of nonspecific autophagy. *Methods Enzymol* 451, 33–42.
- Noda T, Matsuura A, Wada Y, Ohsumi Y (1995). Novel system for monitoring autophagy in the yeast *Saccharomyces cerevisiae*. *Biochem Biophys Res Commun* 210, 126–132.
- Noda T, Ohsumi Y (1998). Tor, a phosphatidylinositol kinase homologue, controls autophagy in yeast. *J Biol Chem* 273, 3963–3966.
- Numrich J, Peli-Gulli MP, Artl H, Sardu A, Griffith J, Levine T, Engelbrecht-Vandre S, Reggiori F, De Virgilio C, Ungermann C (2015). The I-BAR protein Iy1 is an effector of the Rab7 GTPase Ypt7 involved in vacuole membrane homeostasis. *J Cell Sci* 128, 2278–2292.
- Pan X, Roberts P, Chen Y, Kvam E, Shulga N, Huang K, Lemmon S, Goldfarb DS (2000). Nucleus-vacuole junctions in *Saccharomyces cerevisiae* are formed through the direct interaction of Vac8p with Nvj1p. *Mol Biol Cell* 11, 2445–2457.
- Panchaud N, Péli-Gulli M-P, De Virgilio C (2013a). Amino acid deprivation inhibits TORC1 through a GTPase-activating protein complex for the Rag family GTPase Gtr1. *Sci Signal* 6, ra42.
- Panchaud N, Peli-Gulli MP, De Virgilio C (2013b). SEACing the GAP that nEGOCiates TORC1 activation: evolutionary conservation of Rag GTPase regulation. *Cell Cycle* 12, 2948–2952.
- Peterson TR, Laplante M, Thoreen CC, Sancak Y, Kang SA, Kuehl WM, Gray NS, Sabatini DM (2009). DEPTOR is an mTOR inhibitor frequently overexpressed in multiple myeloma cells and required for their survival. *Cell* 137, 873–886.
- Powis K, Zhang T, Panchaud N, Wang R, Virgilio CD, Ding J (2015). Crystal structure of the Ego1-Ego2-Ego3 complex and its role in promoting Rag GTPase-dependent TORC1 signaling. *Cell Res* 25, 1043–1059.
- Reinke A, Anderson S, McCaffery JM, Yates J 3rd, Aronova S, Chu S, Fairclough S, Iverson C, Wedaman KP, Powers T (2004). TOR complex 1 includes a novel component, Tco89p (YPL180w), and cooperates with Ssd1p to maintain cellular integrity in *Saccharomyces cerevisiae*. *J Biol Chem* 279, 14752–14762.

- Sancak Y, Bar-Peled L, Zoncu R, Markhard AL, Nada S, Sabatini DM (2010). Regulator-Rag complex targets mTORC1 to the lysosomal surface and is necessary for its activation by amino acids. *Cell* 141, 290–303.
- Sancak Y, Peterson TR, Shaul YD, Lindquist RA, Thoreen CC, Bar-Peled L, Sabatini DM (2008). The Rag GTPases bind raptor and mediate amino acid signaling to mTORC1. *Science* 320, 1496–1501.
- Sancak Y, Thoreen CC, Peterson TR, Lindquist RA, Kang SA, Spooner E, Carr SA, Sabatini DM (2007). PRAS40 is an insulin-regulated inhibitor of the mTORC1 protein kinase. *Mol Cell* 25, 903–915.
- Sekiguchi T, Hirose E, Nakashima N, Li M, Nishimoto T (2001). Novel G proteins, Rag C and Rag D, interact with GTP-binding proteins, Rag A and Rag B. *J Biol Chem* 276, 7246–7257.
- Sekiguchi T, Kamada Y, Furuno N, Funakoshi M, Kobayashi H (2014). Amino acid residues required for Gtr1p-Gtr2p complex formation and its interactions with the Ego1p-Ego3p complex and TORC1 components in yeast. *Genes Cells* 19, 449–463.
- Sherman F (2002). Getting started with yeast. *Methods Enzymol* 350, 3–41.
- Sikorski RS, Hieter P (1989). A system of shuttle vectors and yeast host strains designed for efficient manipulation of DNA in *Saccharomyces cerevisiae*. *Genetics* 122, 19–27.
- Stone EM, Heun P, Laroche T, Pillus L, Gasser SM (2000). MAP kinase signaling induces nuclear reorganization in budding yeast. *Curr Biol* 10, 373–382.
- Stracka D, Jozefczuk S, Rudroff F, Sauer U, Hall MN (2014). Nitrogen source activates TOR (target of rapamycin) complex 1 via glutamine and independently of Gtr/Rag proteins. *J Biol Chem* 289, 25010–25020.
- Suzuki K, Kamada Y, Ohsumi Y (2002). Studies of cargo delivery to the vacuole mediated by autophagosomes in *Saccharomyces cerevisiae*. *Dev Cell* 3, 815–824.
- Suzuki K, Kirisako T, Kamada Y, Mizushima N, Noda T, Ohsumi Y (2001). The pre-autophagosomal structure organized by concerted functions of APG genes is essential for autophagosome formation. *EMBO J* 20, 5971–5981.
- Urano J, Tabancay AP, Yang W, Tamanoi F (2000). The *Saccharomyces cerevisiae* Rheb G-protein is involved in regulating canavanine resistance and arginine uptake. *J Biol Chem* 275, 11198–11206.
- Urban J, Soulard A, Huber A, Lippman S, Mukhopadhyay D, Deloche O, Wanke V, Anrather D, Ammerer G, Riezman H, et al. (2007). Sch9 is a major target of TORC1 in *Saccharomyces cerevisiae*. *Mol Cell* 26, 663–674.
- Wek SA, Zhu S, Wek RC (1995). The histidyl-tRNA synthetase-related sequence in the eIF-2 alpha protein kinase GCN2 interacts with tRNA and is required for activation in response to starvation for different amino acids. *Mol Cell Biol* 15, 4497–4506.
- Zhang T, Péli-Gulli M-P, Yang H, De Virgilio C, Ding J (2012). Ego3 functions as a homodimer to mediate the interaction between Gtr1-Gtr2 and Ego1 in the EGO complex to activate TORC1. *Structure* 20, 2151–2160.
- Zhao Y, Macgurn JA, Liu M, Emr S (2013). The ART-Rsp5 ubiquitin ligase network comprises a plasma membrane quality control system that protects yeast cells from proteotoxic stress. *Elife* 2, e00459.